Influence of Weather and Surface Variability on Sensible Heat Fluxes in Terra Nova Bay, Antarctica

by

Kelly E. Schick

B.S., Colorado State University, 2014

A thesis submitted to the

Faculty of the Graduate School of the

University of Colorado in partial fulfillment

of the requirements for the degree of

Master of Science

Department of Atmospheric and Oceanic Sciences

2018

This thesis entitled:
Influence of Weather and Surface Variability on Sensible Heat Fluxes in Terra Nova Bay, Antarctica
written by Kelly E. Schick
has been approved for the Department of Atmospheric and Oceanic Sciences

_____
John Cassano

_____
Julie Lundquist

_____
Sharon Stammerjohn

Date _____

The final copy of this thesis has been examined by the signatories, and we find that both the content and the form meet acceptable presentation standards of scholarly work in the above mentioned discipline.

Schick, Kelly E. (M.Sc., Atmospheric Science)

Influence of Weather and Surface Variability on Sensible Heat Fluxes in Terra Nova Bay, Antarctica

Thesis directed by John Cassano

Terra Nova Bay is home to a persistent polynya generated by frequent and intense wind events. Understanding atmospheric processes that influence the sensible heat flux in this region is key to understanding the contribution of the Terra Nova Bay polynya to regional ice production and ultimately Antarctic deep water formation. Automatic weather station (AWS) wind speed and temperature data from Inexpressible Island and surface temperature information is obtained from MODIS Aqua satellite observations over the polynya for the winter season (April to September). Wind speed and temperature data from the years 2003, 2005 and 2012-2017 are used to estimate sensible heat fluxes in Terra Nova Bay using the Coupled Ocean Atmosphere Response (COARE) bulk flux algorithm. Calculated sensible heat fluxes are compared to the input variables of air-surface temperature difference, wind speed, air temperature and surface temperature using rank correlation (ρ). The air$-$surface temperature difference ($\rho = -0.80$) and the wind speed ($\rho = 0.67$) explain a moderate amount of the variance in sensible heat flux with air and surface temperature explaining slightly less ($\rho = -0.41$ and $\rho = 0.53$ respectively). To examine the influence of changing downwind conditions, sensible heat fluxes are then calculated at 10, 20 and 30 km downwind. In order to best modify the AWS observations to correspond with the downwind distances, gradients of air temperature and wind speed are calculated using Unmanned Aerial System (UAS) observations made over Terra Nova Bay in September 2009 and 2012. The resulting average hourly upward heat flux decreases from 457.8 W m^{-2} at the coast to 163.6 W m^{-2} 30 km downwind. Monthly mean sensible heat flux varies from 328.9 W m^{-2} in September to 511 W m^{-2} in August. The incidence of statically unstable conditions decreases over that same distance from 89% to 78%. Hourly sensible heat fluxes were used to estimate hourly ice growth rates which decrease from 0.8 cm h^{-1} near the coast to 0.3 cm h^{-1} 30 km downwind. These hourly rates convert to seasonal ice growth estimates

of 30 m near the coast and 9m 30 km downwind from the coast.

Acknowledgements

The author thanks the University of Wisconsin Antarctic Meteorological Research Center for providing the Inexpressible Island AWS data. The satellite surface temperature data was provided by the National Snow & Ice Data Center. This research was supported by NSF grant PLR 1341606.

In addition, the author extends thanks to her advisor, John Cassano, for supporting and pushing her as needed, and providing the opportunity to not only complete the following work, but to travel to Antarctica as part of the 2017 PIPERS project and experience the unique environment described in this work. There are many other people who have been generous with their time during this project, especially my committee members Julie Lundquist and Sharon Stammerjohn. Both have provided an immense amount of support and encouragement throughout the writing of this document. All of the members of the Cassano group are thanked for providing support, encouragement and fun anecdotes over my three years with the group. Finally, all of the wonderful students at the University Lutheran Chapel who have worked to keep me focused and sane throughout the writing of my thesis.

Contents

Tables

Table

Figures

Figure

Chapter 1

Background

Polynyas, regions of open water surrounded by sea ice, are influential locations for heat exchanges, ice production and deep water formation. Large differences observed between atmosphere and ocean surface conditions lead to large upward sensible heat fluxes ([Knuth and Cassano, 2014]). Terra Nova Bay, located in the southwestern Ross Sea, is home to a persistent polynya shaped by the frequent and intense off-continent wind flow where the air sea heat exchange is known to be particularly large in winter ([Fusco et al., 2002]). The extent of the polynya can be defined as the distance between open water with frazil formation to the location at which the ice cements together and begins to act as a solid body ([Martin and Kauffman, 1981]). The polynya area varies throughout the winter season from 3000 to 7000 km^2 ([Hauser et al., 2002]). The north south extent of the Terra Nova Bay polynya is defined by the Drygalski Ice Tongue to the south and the continent to the north and west(Figure 1).

Strong, off continent surface winds exist in the region due to the confluence of outflow over the Reeves and Priestley Glaciers ([Parish and Bromwich, 2007], [Kurtz and Bromwich, 1985]). The strong winds common in Terra Nova Bay are often katabatic winds, driven by radiative cooling of the air on the Antarctic Plateau. The cooled air is driven down into glacial valleys creating a funneling effect leading to the intense wind speed observed in the area ([Davolio and Buzzi, 2002]). The forcing that drives the katabatic winds is slightly weaker in the summer (December to February) than in the winter season (April to September) ([Parish and Cassano, 2003]). The strength of upper level pressure gradients will influence the strength of the downsloping flow, with steeper

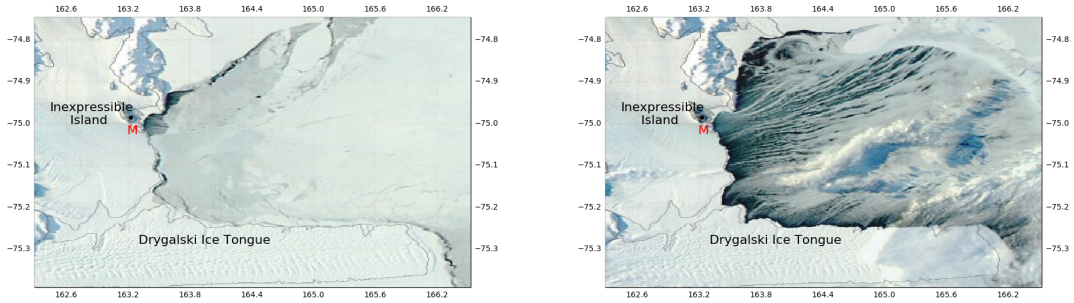

(a) (b)

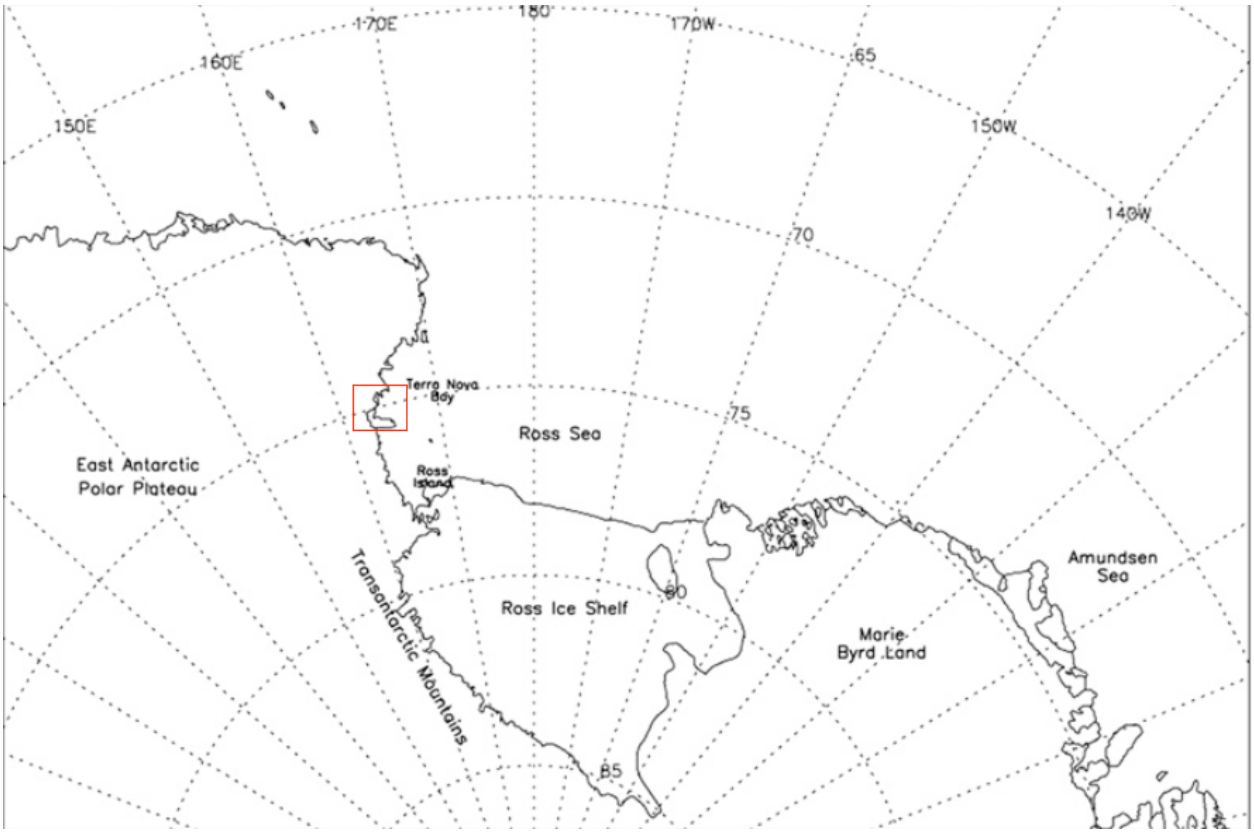

(c)

Figure 1: Aqua visible satellite imagery of Terra Nova Bay on 18 September 2012, showing the polynya to be primarily sea ice covered (a) and 25 September 2012, after the opening of the polynya due to katabatic winds (b). Approximate location of Manuela AWS on Inexpressible Island is noted in red. Visible imagery is obtained from NASA WorldView at the 250 m resolution. Location of Terra Nova Bay in the context of the greater Antarctic continent is show in (c) adapted from Knuth and Cassano 2011. Approximate location of satellite imagery is show by box in red.

pressure gradients aloft enhancing the near surface flow ([Knuth and Cassano, 2011]).

Cold, dry air blowing off the continent interacts with the ocean surface to almost instantly create sea ice in the region. Sea ice growth is directly proportional to the sensible heat flux through the product of the latent heat of fusion, which is dependent of the oceanic state parameters of temperature and salinity as well as ice density. Almost all ice formed is advected to the eastern edge of the bay due to the strong winds. Advection of ice, from the south, into Terra Nova Bay is almost completely blocked by the Drygalski Ice Tongue to the south. Cold high salinity, and thus dense, water is created through the rapid production of sea ice. This dense water is the basis for the formation of Antarctic deep water ([Ohshima et al., 2016]).

Observations of the region are available from a variety of sources including satellite, automatic weather station, unmanned aerial system and ship-based measurements. The University of Wisconsin automatic weather station (AWS) network has been in place from the early 1980s collecting hourly atmospheric state measurements for multiple Antarctic locations, including the Manuela station (74.9 S 163.7 E) on Inexpressible Island in Terra Nova Bay ([Lazzara et al., 2012]). The NASA Earth Observing System Terra and Aqua satellites provide nearly daily overpasses of the region collecting multiple types of observations including MODIS derived surface temperatures ([Hall and Riggs, 2015a] and [Hall and Riggs, 2015b]). Unmanned aerial system (UAS) flights ([Cassano et al., 2010]; [Knuth et al., 2013]) and ship-based observations provide in situ data of the polynya itself. In the work described below AWS, UAS and satellite observations are used to calculate sensible heat fluxes over the Terra Nova Bay polynya during the winter season using the Coupled Ocean Atmosphere Response (COARE) flux algorithm ([Fairall et al., 1996]).

The COARE flux algorithm was developed out the desire to parameterize air-sea turbulent fluxes after the 1992 field campaign of the same name ([Fairall et al., 1996]). Originally developed as a bulk algorithm to be used in the tropics, desire to use the algorithm to characterize air-sea interactions in other regions lead to the 2003 release of a globalized algorithm that uses local observations to calculate physical variables whenever possible. Among the updates in version 3.0 are improvements to the stability function, a change in wind speed dependences to transfer coef-

ficients above 10 m s^{-1} and a reduction to the stability iteration of the heat transfer coefficient ([Fairall et al., 2003]).

The ultimate goal of understanding the variability in sensible heat flux is to better quantify the variability in ice production in Terra Nova Bay. Section 2 of this paper describes the three data sources used in this research. Section 3 presents the methodology, while section 4 presents the results and discussion. A summary of the work is given in section 5.

Chapter 2

Data

Three sources of data are used to calculate sensible heat fluxes over the Terra Nova Bay polynya: AWS observations are used to define the atmospheric state, satellite data is used to specify surface conditions and UAS data is used to estimate how the atmospheric state varies with downwind distance over the polynya. Sensible heat fluxes are only calculated when data from both the AWS and satellite observations are available. Both datasets are available for the winter seasons (defined here as April to September) of 2003, 2005 and 2012-2017 for a total of over 35,000 hours of observations.

2.1 Automatic Weather Station

The University of Wisconsin AWS network has been successfully reporting data from the Antarctic for over 30 years ([Lazzara et al., 2012]). For this project, the AWS of interest is Manuela located on the southern edge of Inexpressible Island at the head of Terra Nova Bay (Figure 1). The AWS data are used to specify the atmospheric state, with temperature and wind speed being the primary variables of interest. Sensors mounted on a 3 m tower have been installed on Inexpressible Island since 1984. Data are transmitted hourly via the ARGOS network. Data are quality controlled by the University of Wisconsin and are provided at 10-minute, 1-hourly and 3-hourly resolution. For the purposes of this project, 1-hourly data are used to provide sufficient resolution for the variation in wind strength in Terra Nova Bay. The AWS Temperature sensors are reported to have an accuracy of ± 0.2 K, with little observed drift over the lifetime of the instrumentation

([Lazzara et al., 2012]). Wind speed measurements are a particular challenge at the Manuela station due to its location in an area of strong katabatic outflow. After many years with wind sensors failing over the winter season (when winds are strongest), the wind sensor at the Manuela AWS was switched to a Hydro-Tech sensor which provides the ability to withstand the hurricane-strength winds experienced at Manuela at the expense of some accuracy at low wind-speeds. Accuracy for this sensor is reported in general as $\pm$ 2%. For the purpose of this project, wind speeds below 1 m s^{-1} are considered suspect in terms of accuracy due to the frequency that these values occur during periods when the data is otherwise flagged as questionable by the University of Wisconsin quality control process. Additionally, these light wind speeds are not supported by the climatology of the region ([Knuth and Cassano, 2011]).

2.2 Satellite Observations

Surface temperature data is obtained from the thermal infrared bands of the NASA Earth Observing Systems (EOS) Aqua satellite-borne Moderate Resolution Imaging Spectroradiometer (MODIS) ([Hall and Riggs, 2015a],[Hall and Riggs, 2015b]). Launched in 2002, Aqua MODIS views the entire Earth's surface every 1 to 2 days, acquiring data in 36 spectral bands. Scambos et al (2006) found the root mean square error of the temperature data to be 1 K. The data is gridded to the EASE (Equal-Area Scalable Earth) grid providing two observations per UTC day, defined as day or night by the amount of daylight present. During a portion of the winter season (May through July), there are no day observations available and only night observations are considered. Observations that are obscured with cloud are also not included in this analysis at the satellite cannot observe the surface. Data is included from the April to September winter season for the years 2003, 2005, and 2012-2017. Coastal satellite surface temperature observations were taken from a satellite grid cell roughly 2 km from the location of the AWS. This point was chosen to minimize the distance from the Manuela AWS in the downwind direction while also ensuring that the site was an oceanic, not land covered, grid point. Additional satellite grid points further off-shore in the predominant downwind direction were selected to be 10, 20, and 30 km from the coastal grid

point.

2.3 Unmanned Aerial Systems Observations

UAS flights conducted in September 2009 and 2012 utilized the Aerosonde unmanned aerial system ([Knuth and Cassano, 2011]; [Knuth et al., 2013]; [Cassano et al., 2016]). On board sensors measured air temperature, pressure, wind speed, position and surface temperature. Flights were conducted from Pegasus Runway, located near McMurdo Station, and flew along the coast of Victoria Land across the Drygalski Ice Tongue to Terra Nova Bay. For the purposes of this project, only the flights that were aligned with the katabatic jet core are considered. The data from level flight segments (altitude of roughly 110 m above ground level) aligned with the wind direction are utilized to calculate downwind differences in air temperature and wind speed. Air temperature observations are recorded at 5 second resolution with a temperature dependent accuracy reported as $\pm$ (0.226 - 0.0028 x measured temperature) ([Cassano et al., 2016]). Wind speed and wind direction are determined from the UAS operating systems measurements of ground speed, track, and true air speed with a reported accuracy of 1 m s^{-1}.

Chapter 3

Methods

The primary method of analysis in this paper utilizes the COARE algorithm to calculate sensible heat fluxes from a combination of AWS and satellite data. Relations between the sensible heat flux and atmospheric and surface parameters are investigated using the non-parametric Spearmans Rank Correlation. Sensible heat fluxes are then calculated at three downwind distances after modifying the AWS data using downwind differences calculated from UAS flights. Finally, hourly averaged sensible heat fluxes are converted into hourly, monthly and seasonal ice production estimates.

3.1 Sensible Heat Flux Calculations

Sensible heat fluxes in this project are calculated using the COARE algorithm (v. 3.0). Originally developed for use in tropical ocean conditions, in version 3.0 the algorithm has been expanded to allow for more global use, including polar conditions, by incorporating observed conditions to calculate physical variables whenever possible (Fairall et al 2003). Fairall et al (2003) found the accuracy of the algorithm to be within 5% at wind speeds less than 10 m s^{-1} and within 10% for wind speeds from 10 to 20 m s^{-1}. It should be noted that the conditions observed during this project are frequently outside of that given range and may affect the accuracy of calculations performed with wind speeds in excess of 20 m s^{-1}. The sensible heat flux (SHF) is calculated using the basic formula:

$$SHF = \rho c_p C_H U (T_{SFC} - T). \quad (1)$$

Here, ρ is the density of air, c_p is the specific heat of air at constant pressure, U is the wind speed, T_{SFC} is the surface temperature, T is the air temperature and C_H is the bulk transfer coefficient. The COARE flux algorithm uses an iterative method to estimate the bulk transfer coefficient based on a combination of the transfer coefficient for temperature and wind speed. The algorithm reaches stability for the transfer coefficients in three iterations. Wind speed and air temperature inputs are obtained for coastal calculations from the AWS observations and from the AWS observations modified with UAS estimated downwind gradients from five flights over Terra Nova Bay as discussed below. Surface temperature data is obtained from MODIS Aqua satellite observations as described previously in the Data section of this paper.

3.2 Spearmans Rank Correlation

Spearmans rank correlation is a non-parametric test that evaluates whether or not two data vary monotonically with each other. The variation does not have to be linear, and the data do not have to be normally distributed. Data are converted into ranks of descending order Xi and Yi, with mean $\bar{X}$ and $\bar{Y}$. The rank correlation is calculated as:

$$\rho = \frac{(X_i \bar{X})(Y_i - \bar{Y})}{\sqrt{(X_i \bar{X})^2 (Y_i - \bar{Y})^2}} \tag{2}$$

When comparing the sensible heat flux to atmospheric and surface state parameters, we do not expect a linear relation nor for the data to be normally distributed. In particular the wind speed observations for the eight winter seasons do not follow a normal distribution (Figure 2d). Thus, we choose the Spearmans Rank Correlation to evaluate the relative strength of the relationship between the sensible heat fluxes and the atmospheric and surface state parameters. Values of Spearmans Rank Correlation range from -1 to +1 where positive values indicate a positive correlation, and negative values indicate a negative correlation. Higher magnitude values indicate a stronger correlation with values around $\pm$ 0.5 indicating a moderate correlation.

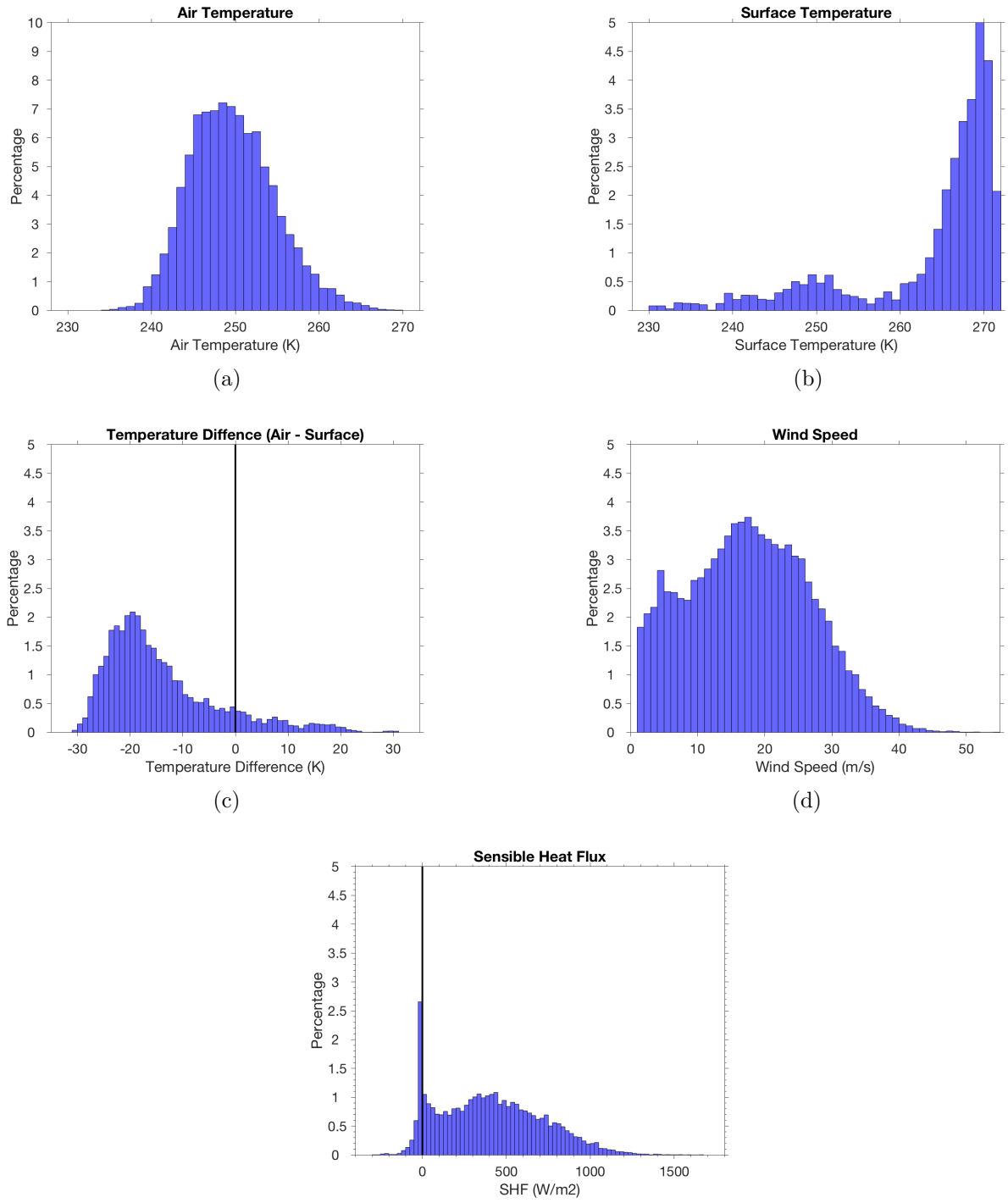

Figure 2: Observed air temperature (a), surface temperature (b), temperature difference (air surface) (c), wind speed (d) at Manuela AWS on Inexpressible Island for April to September of the years 2003, 2005 and 2012-2017. Calculated sensible heat fluxes (SHF) (e) based on Manuela AWS and MODIS Aqua observations for the same time period.

3.3 UAS Modifications to AWS Observations

Observations from five UAS flight days over Terra Nova Bay during September 2009 and September 2012 ([Cassano et al., 2010]; [Cassano et al., 2016]) are used to make estimates of the average change in air temperature and wind speed at 10, 20 and 30 km downwind from the coast. Data from flight segments aligned with the katabatic jet core when the UAS maintained a constant altitude and heading are used to perform a linear regression between distance and air temperature or wind speed. Separate fits are conducted at 10, 20 and 30 km downwind. The slope of the linear regression is then multiplied by the desired distance (e.g., 20 km) to achieve the downwind differences shown in Table 1. These differences are then used to modify the AWS observations before input into the COARE algorithm as described below in the results section.

3.4 Conversion from Sensible Heat Flux to Ice Growth

The ultimate goal of understanding the variability in sensible heat flux is to better quantify the variability in sea ice production in Terra Nova Bay. To this end, a conversion is performed between hourly sensible heat fluxes and hourly sea ice growth rate at each distance (coastal and 10, 20 and 30 km downwind) and each month of the winter season (April through September). To convert from sensible heat flux to ice production, reasonable values for the latent heat of fusion and the density of freshly formed Antarctic sea ice (pancake ice) are needed. The latent heat of fusion depends on the ocean salinity and surface temperature of the ocean. Typical ocean surface temperatures during the winter season are roughly 271 K with 10 ppt salinity. With these values the latent heat of fusion is calculated to be 2.36 x 10^5 J kg^{-1} for pancake ice with density of 922 kg m^{-3} ([Ono, 1967]). To calculate monthly and seasonal estimates of ice production the number of hours in a given month is multiplied by the fraction of observations classified as unstable. It is assumed that invalid observations demonstrate the same stability behavior as the valid observations. The estimated total number of monthly or seasonal statically unstable hours is then multiplied by the monthly or seasonal average hourly upward sensible heat flux. The resulting sensible heat content

is then converted into ice production by dividing by the product of the latent heat of fusion and density described above.

Chapter 4

Results

The observations from eight winter seasons at Manuela station on Inexpressible Island illustrate the range of unique conditions that occur in Terra Nova Bay. As illustrated in Figure 2a, the air temperatures range from 235 K to near 270 K with the majority in the 245 to 255 K range. Figure 2b illustrates the surface temperature distribution observed near the coast on the lee of Inexpressible Island. The peak in observation frequency occurs at 269 K. This temperature is associated with thin ice or open water, temperatures above this value are likely to indicate open water with temperatures below this value indicating the presence of ice. The distribution indicates that near the area near the coast is often nearly open rather than ice covered (1a and 1b). Combining the air and surface temperature data at matching times results in an air-surface temperature difference ranging from -30 to 30 K, as shown in Figure 2c. The peak of observation frequency of the temperature difference distribution falls around -20 K. The majority of observations are negative indicating that the surface is warmer than the air generating statically unstable conditions. The majority of the conditions in Terra Nova Bay will therefore generate an upward (positive) sensible heat flux.

Observed wind speeds range from quiescent at 1 m s^{-1} to the extreme range at over 50 m s^{-1}as shown in Figure 2d, with 17 m s^{-1} being the most commonly observed value. The majority of the winds in Terra Nova Bay are associated with downslope and off continent flow, with deviations from that wind direction occurring for lighter wind speeds ([Knuth and Cassano, 2011]). The predominance of strong winds is associated with the strong katabatic jets or other downsloping

wind patterns that dominate the region.

Sensible heat fluxes were calculated with the COARE algorithm using the observed atmosphere and surface state discussed above. Upward fluxes here are defined as those that occur during statically unstable conditions where the surface is warmer than the air and thus heat is transferred upward from the ocean surface to the atmosphere. Downward fluxes occur when the atmosphere is statically stable and heat is transferred downward from the atmosphere to the ocean surface. The calculated sensible heat flux is proportional to the wind speed, the surface to air temperature difference and a stability correction which depends on both of these quantities as shown in Eq.1. The spread of the positive, upward sensible heat fluxes (Figure 2e) is similar to the wide and relatively flat distribution observed in the wind speed distribution (Figure 2d), with the exception of the peak in observed frequency of small, but non-negative sensible heat fluxes. The majority of downward fluxes occur in the small, near zero values illustrated as negative values in Figure 2e. The focus of the remainder of this paper will be on variations in the upward sensible heat fluxes due to weather and surface conditions since these are the conditions that are of interest for ice production.

To understand the combination of atmosphere and surface conditions that give rise to the range of sensible heat fluxes seen in Figure 2e we have calculated Spearmans Rank Correlation (2) for the atmospheric and surface state variables in relation to the sensible heat flux. As expected, the upward sensible heat flux increases as the temperature difference becomes more negative, a negative correlation of ρ =-0.80 (Figure 3a). The variation about that negative correlation can be explained by the variation in wind speed for a given temperature difference as illustrated by the color bar in Figure 3a. Higher wind speeds (as indicated by the color bar) result in larger fluxes for a given temperature difference. As expected, a positive correlation exists between the sensible heat flux and the wind speed (ρ=0.67; Figure 3b). This shows that the variation in sensible heat flux at a particular wind speed is explained by variation in the air-surface temperature difference, with larger fluxes occurring for a given wind speed when the temperature difference is larger. While the value of ρ = -0.80 is slightly larger for the sensible heat flux to temperature difference relation than the sensible heat flux to wind speed relation (ρ = 0.67) both indicate a moderately strong

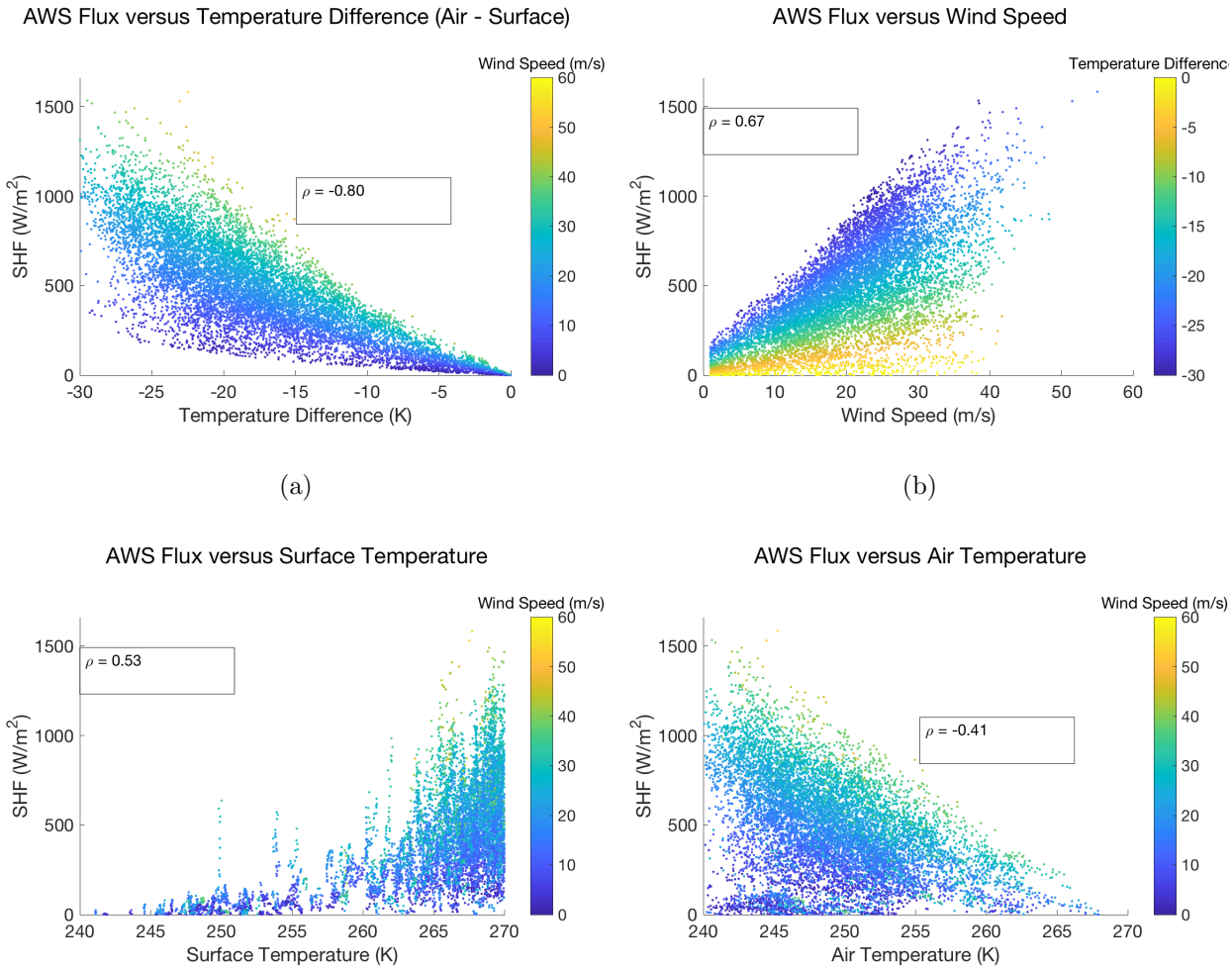

Figure 3: Influence of air-surface temperature difference (a), wind speed (b), coastal ocean surface temperature (c), and air temperature (d) on calculated sensible heat flux. The corresponding Spearman rank correlation is printed on each panel. Scatter plot color indicate wind speed in panels (a), (c) and (d) and air-surface temperature difference in panel (b).

correlation. Weaker correlations exist for sensible heat flux to surface and air temperature with values of ρ = 0.53 and ρ= -0.41 (Figures 3c and 3d) respectively. While a monotonic relationship is expected from the nature of the COARE algorithm, the overall spread about the monotonic relationship demonstrates the independent variations possible in each atmospheric state parameters. While there is no clear linear trend, the Spearmans Rank correlation indicates the presence of a monotonic increasing or decreasing relationship. This indicates that surface and air temperature variability account for a similar amount of the overall sensible heat flux variability, and less so than the air-surface temperature difference and wind speed. Wind speed is used for the color bar in Figure 3c and 3d, where increasing wind speed is correlated with a higher sensible heat flux at a set value of air or surface temperature. While the causes of wind variability are beyond the scope of this paper, the effects of changing surface conditions and downstream air parcel modification on the sensible heat flux will be investigated to better understand the impact of the heat flux variability on ice production in Terra Nova Bay.

Satellite observations of surface temperature shows an increase in the temperature of the peak of the distribution from the coast to 10 km (Figures 4 4a and 4c) followed by a decrease in the surface temperature peak as distance away from the coast increases (Figures 4c, 4e and 4g). The increase from the coast to 10 km is a result of the presence of fast ice in the satellite observation pixel near the coast that is not present 10 km downwind. As a result, open water, and thus warmer surface temperatures, are more often observed at the 10 km downwind distance than immediately adjacent to the coast. The difference in fast ice extent near the AWS location with can be seen in Figure 1a demonstrating further southward progression of the fast ice than a week later in Figure 1b. The decrease in the temperature at the peak of the distribution with distances beyond 10 km downwind of the coast is likely due to the effects of the strong offshore flow advecting sea ice away from the coast and near coastal regions. This creates a region with more sea ice and cooler temperatures further away from the coast ([Sansiviero et al., 2017]) as observed by the decreasing surface temperature peak from 10 to 30 km in Figures 4c and 4g respectively. For the coastal, 10 and 20 km observations the most frequently occurring temperature values are in the range of 267 to

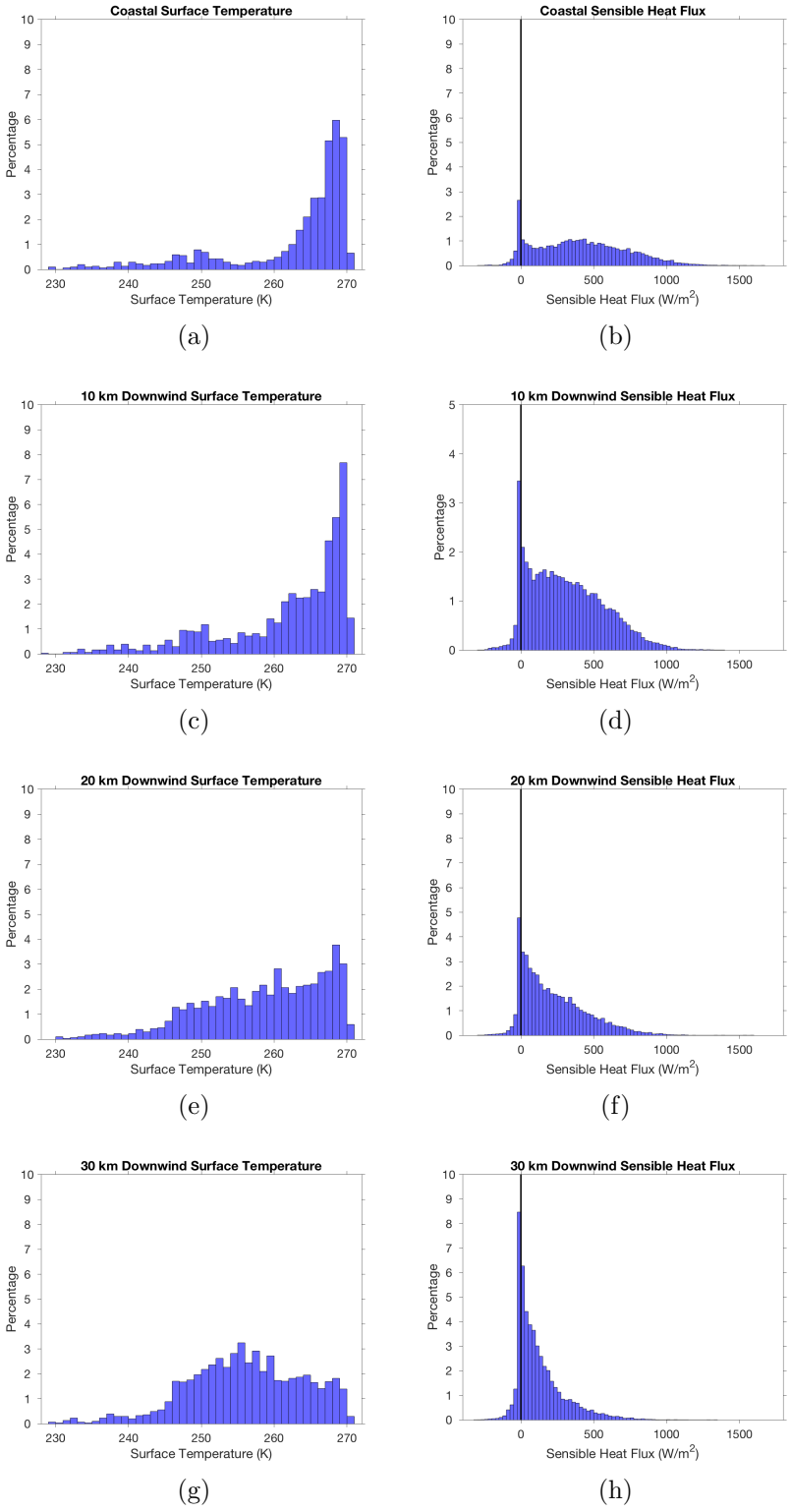

Figure 4: Histograms of satellite surface temperatures (panels a, c, e, and g) and sensible heat fluxes (panels b, d, f, and h) at the coastal (panels a and b) and distances of 10 km (panels c and d), 20 km (panels e and f), and 30 km (panels g and h) downwind from the coast of Inexpressible Island.

271 K indicative of the nearly completely open water of the polynya. However, the distribution of surface temperatures shifts with the downwind distances to have more frequently occurring colder temperatures. Figure 4g shows that by 30 km downwind the majority of temperature fall in the mid 250 K range illustrating that at this distance the sea surface is more likely to be ice covered and cold.

In order to accurately estimate the sensible heat flux the atmospheric conditions, as represented by the AWS observations at the coast, must be extrapolated to the desired downwind distance. It is expected that as the air mass moves downstream it will warm due to the upward sensible heat flux and for the wind speed to decrease due to momentum loss to the surface through turbulence. To appropriately estimate how much the observed wind speed and temperature will change as the continental air mass moves further offshore, data from five UAS flights aligned with the katabatic jet core on five different days (two in September 2009 and three in September 2012) are used ([Knuth et al., 2013], [Cassano et al., 2016]). The ranges of the UAS downwind changes in temperature and wind speed are listed in Table 1. On average, the air temperature warms 1 K and the wind speed decreases 2.6 m s^{-1} when moving 10 km downwind from the coast of Inexpressible Island. These values increase in magnitude as distances further downstream are considered. Satellite observations of surface temperature for the same five flight days were used to calculate the

	Air Temperature Change (K)			Surface Temperature Change (K)			Wind Speed Change (m s^{-1})		
	Minimum	Maximum	Average	Minimum	Maximum	Average	Minimum	Maximum	Average
10 km	0.3	2.5	1.0	5.5	13.2	8.8	-6.1	0.4	-2.6
20 km	-1.4	2.8	1.1	-5.1	0.0	-2.1	-7.4	-1.1	-3.7
30 km	2.2	3.4	2.9	-7.9	-0.8	-3.3	-6.8	-3.4	-5.5

Table 1: The minimum, maximum and average difference of air temperature, surface temperature and wind speed from the coast to 10 km, 20 km and 30 km downwind from Inexpressible Island. Air temperature and wind speed differences are calculated using UAS observations from 5 flight days in September 2009 and 2012, with surface temperature differences are calculated using satellite observations on those same days.

surface temperature difference between the coast and 10, 20, and 30 km downstream to provide a comparison with the UAS observed air temperature differences. The surface temperature on these days increases, on average, by 8.8 K over the first 10 km downwind of the coast and then decreases 2.1 to 3.3 K over the next 20 km. The large positive 10 km surface temperature difference shown in Table 1 is a result of the thicker and therefore colder ice present near the coast in the satellite observation pixel on the leeward side of Inexpressible Island on the five UAS flight days. If satellite observations over all eight winters are considered instead of just the flight days, the 10 km downwind surface temperature difference is -1.1 K indicating the expected progression from warmer to colder surface temperature downstream exists on average. Air temperature varies slightly less with downstream distance compared to the surface temperature in terms of magnitude and spread, emphasizing the importance of surface temperature variability on the sensible heat flux. Based on the downstream differences of temperature and wind speed given in Table 1 we can extrapolate the AWS conditions at Inexpressible Island to distances 10, 20 and 30 km downwind from the coast. Using these extrapolated AWS values with the satellite observed surface temperatures from the same days as the AWS observations allows sensible heat fluxes to be calculated downwind from the coast of Terra Nova Bay.

The impact of using the minimum, maximum and average observed downwind difference of air temperature and wind speed from Table 1 applied separately and in combination to the AWS data are shown Figure 5. For the temperature difference (Figure 5a), the distribution of values is shifted to less negative values with each increase in applied downstream difference. This indicates that downstream warming of the air parcel reduces the air to surface temperature difference, thus reducing the resultant sensible heat flux slightly (Figure 5b). The resulting sensible heat flux variation from only modifying the air temperature is minimal. There is a slight increase in the small, but still positive sensible heat fluxes near zero when considering the average change (dashed line) in relation to the distribution with no applied change (black line). The distribution remains largely unchanged with the minimum and maximum applied changes, indicating that the sensible heat flux is not sensitive to the downwind air temperature gradient applied. The values calculated from the

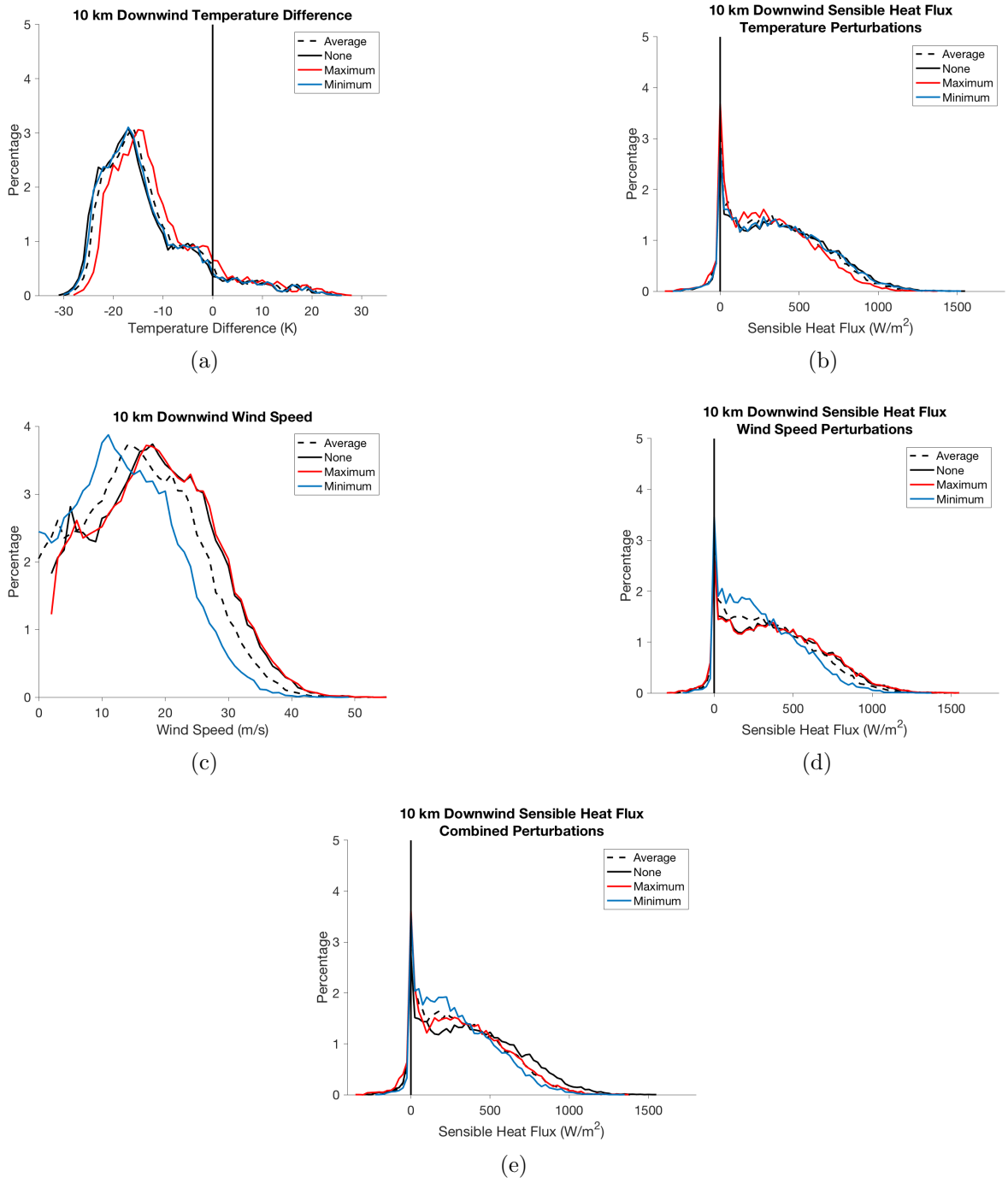

Figure 5: Effects of wind speed and temperature difference on downwind sensible heat fluxes. Histogram show spread of 10-km downwind (a) air-surface temperature difference distribution after the application of 4 gradients: none (solid black line), maximum (red), minimum (blue) and average (dashed black line), (b) the calculated sensible heat flux that results from the temperature difference variations in combination with the observed surface temperature, (c) the wind speed distribution with 4 gradients applied: none (solid black line), maximum (red), minimum (blue) and average (dashed black line), (d) the resulting sensible heat flux from the wind speed variations in combination with the observed surface temperature and (e) the sensible heat flux that results from applying the temperature and wind speed variations in combination (none (solid black line), maximum (red), minimum (blue) and average (dashed black line)).

maximum and minimum air temperature downwind differences are vary only slight from those calculated using the average air temperature downwind difference and observed surface temperature in the sensible heat flux distribution.

Applying the wind speed downwind difference produces an increase in the frequency of lower wind speed values (Figure 5c). A peak in distribution now occurs at 11 or 12 m s^{-1} for the minimum and average gradient respectively as opposed to the 17 m s^{-1} peak frequency seen at the coast. This reduction in wind speed reduces the magnitude of the sensible heat flux with a decrease in sensible heat fluxes above 500 W m^{-2} and an increase in frequency for sensible heat fluxes below 300 W m^{-2} (Figure 5d) when comparing the no applied change (black line) to the average applied change (dashed line). When the temperature and wind speed gradients are applied in combination, the change in sensible heat flux distribution is similar to that seen when only the wind speed variation was considered (Figures 5d and 5e). This indicates that the downwind change in the sensible heat flux is more sensitive to the wind speed downwind difference than the air temperature downwind difference based on data from the five UAS flight days.

Applying the average air temperature and wind speed differences with the satellite observed surface temperatures at multiple downwind distances allows for the estimation of sensible heat fluxes over Terra Nova Bay. While Figure 5 only illustrates the impact of air temperature and wind speed differences over the first 10 km from the coast on the calculated fluxes, similar trends are observed at 20 and 30 km downwind when the differences shown in Table 1 are used to estimate the sensible heat fluxes at these distances. As was noted at 10 km downwind the largest impact on the sensible heat fluxes moving downwind over Terra Nova Bay is the changing surface temperature differences.

Since the average temperature and wind speed downwind differences capture the majority of the variability generated by downstream changes in the atmospheric state (Figure 5), the combined average perturbations are used to estimate the distribution of sensible heat fluxes at several distances downwind from the coast (Figures 4d, 4f, 4f, and 4h). The magnitude and range of positive sensible heat fluxes becomes smaller with increasing downwind difference. The average hourly up-

ward flux decreases from 457.8 W m^{-2} to 163.56 W m^{-2} over the 30 km distance (Table 2, Figure 6). Despite the increase in ice cover and decrease in surface temperature with distance away from

	Valid	Stability		Hourly Sensible Heat Flux (W m^{-2})		Hourly Ice Growth	Seasonal Ice Growth
		Unstable	Stable	Upward	Downward	(cm hr^{-1})	(m)
Coastal	36%	89%	11%	457.8	23.6	0.8	30
10 km Downwind	47%	90%	10%	348.4	22.9	0.6	23
20 km Downwind	50%	87%	13%	259.4	22.0	0.4	16
30 km Downwind	53%	78%	22%	163.6	20.5	0.3	9

Table 2: The downwind variation in valid data available, stability conditions split into statically unstable and stable, hourly sensible heat flux split into upward (resulting from statically unstable conditions) and downward (resulting from statically stable conditions) in W m^{-2}, hourly ice growth in cm h^{-1} and seasonal ice growth in m at locations near the coast and 10,20 and 30km downwind.

the coast, the atmosphere over Terra Nova Bay remains largely in the statically unstable regime (78 to 90% of the time) with heat being transferred from the ocean and sea ice to the atmosphere (Table 2, Figure 6). The largest upward heat fluxes decrease from in excess of 1000 W m^{-2} at the coastal point to less than 850 W m^{-2} 30 km from the coast (Figure 4). Thus, not only do the upward fluxes decrease in frequency as a result of the decrease in statically unstable conditions, they decrease in magnitude. The frequency of negative (downward) sensible heat fluxes increases with downward distance (Figures 4b, 4d, 4f and 4h) indicating a corresponding increase to the percentage of stable conditions as the surface temperature cools and atmosphere warms at 20 and 30 km downwind (Table 2, Figure 6). The magnitude of the downward flux from the coast to 30 km downwind is largely unchanged at roughly 20 W m^{-2}, although these downward fluxes occur more often as indicated by the increasing frequency of stable conditions (Figure 6, Table 2). The average upward flux is much larger in magnitude than the average downward hourly flux (Table 2, Figure 6). This difference in magnitude supports the importance of understanding the variability of the upward sensible heat flux.

The upward sensible heat flux is particularly important when considering sea ice production in the Terra Nova Bay polynya. Using the value put forth in the methods section of the latent

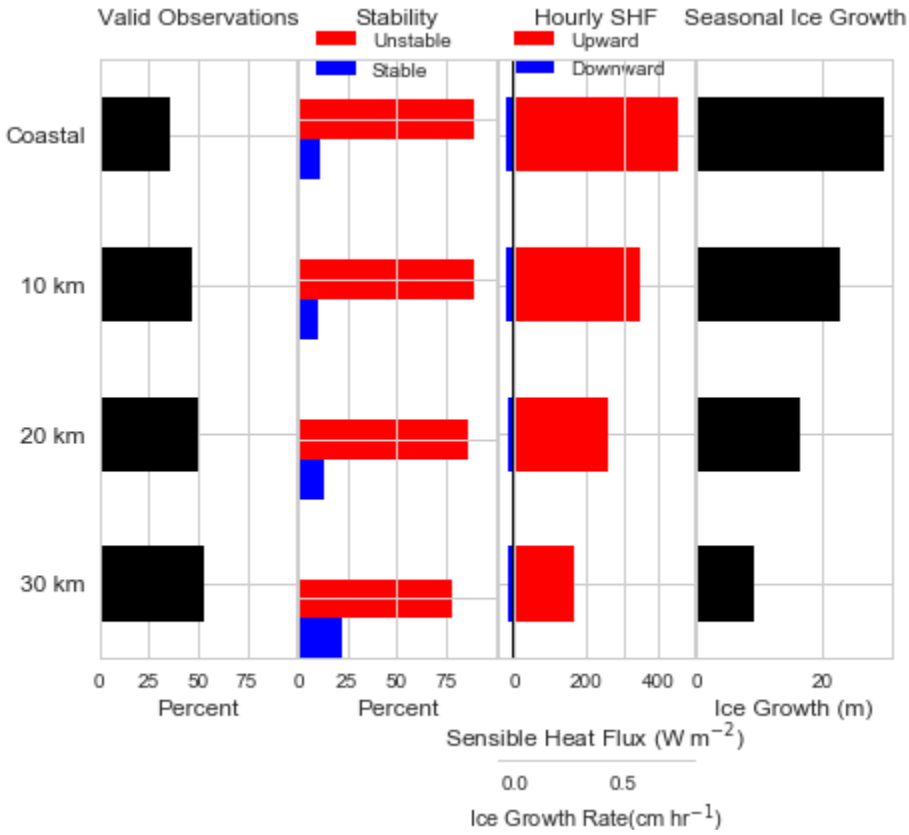

Figure 6: Bar charts representing the percentage of data valid (a), the stability conditions with unstable conditions in red and stable conditions in blue (b), the hourly sensible heat flux in W m^{-2} and ice growth rate in cm h^{-1} with red representing upward (positive) fluxes and blue representing downward (negative) fluxes (c) and the seasonal ice growth in m (d) near the coast and at distances 10, 20 and 30 km downwind.

	Valid	Stability		Hourly Sensible Heat Flux (W m^{-2})		Hourly Ice Growth (cm hr^{-1})	Monthly Projected Ice Growth (m)
		Unstable	Stable	Upward	Downward		
April	30%	88%	12%	452.4	25.6	0.7	5
May	51%	86%	14%	424.5	13.5	0.7	4
June	47%	91%	9%	497.5	17.4	0.8	5
July	37%	82%	5%	424.6	9.8	0.7	4
August	19%	80%	20%	511.0	31.8	0.8	5
September	26%	87%	13%	328.9	21.5	0.5	3

Table 3: The monthly variation in valid data available, stability conditions split into statically unstable and stable, hourly sensible heat flux split into upward (resulting from statically unstable conditions) and downward (resulting from statically stable conditions) in W m^{-2}, hourly ice growth cm h^{-1} and monthly projected ice growth in m.

heat of fusion for typical Antarctic conditions the hourly sensible heat fluxes can be converted into hourly ice production estimates. At the coast, the hourly ice growth rate is 0.8 cm h^{-1} decreasing to 0.3 cm h^{-1} 30 km down wind. Using the frequency of unstable conditions, and the total number of hours in each month, the monthly ice growth due to the upward heat fluxes can be estimated. This yields a projected 30 m of ice grown near the coast over the April to September winter season, decreasing to a projected 23 m of seasonal ice growth at 10 km, 16 m at 20 km and 9 m at 30 km downwind (Figure 6, Table 2).

The variation of stability, sensible heat flux and ice growth at the coast can also be broken out by month over the winter season as shown in Table 3 and Figure 7. The percentage of unstable observations ranges from 80 to 90%, with August having the fewest unstable observations and June having the largest percentage of unstable cases. Hourly upward sensible heat flux values range from 328.9 W m^{-2} in September to 511.0 W m^{-2} in August. With the exception of September with an hourly ice growth of 0.5 cm h^{-1}, the sensible heat fluxes convert to hourly ice growth rates ranging from 0.7 to 0.8 cm h^{-1}. This results in an estimate of 4 to 5 m of projected monthly ice production. This indicates little month to month variability in the contribution to the seasonal ice growth total, although September produces a slightly smaller projected amount of ice (3 m) than the other months. Hourly downward sensible heat flux values show more month to month variation

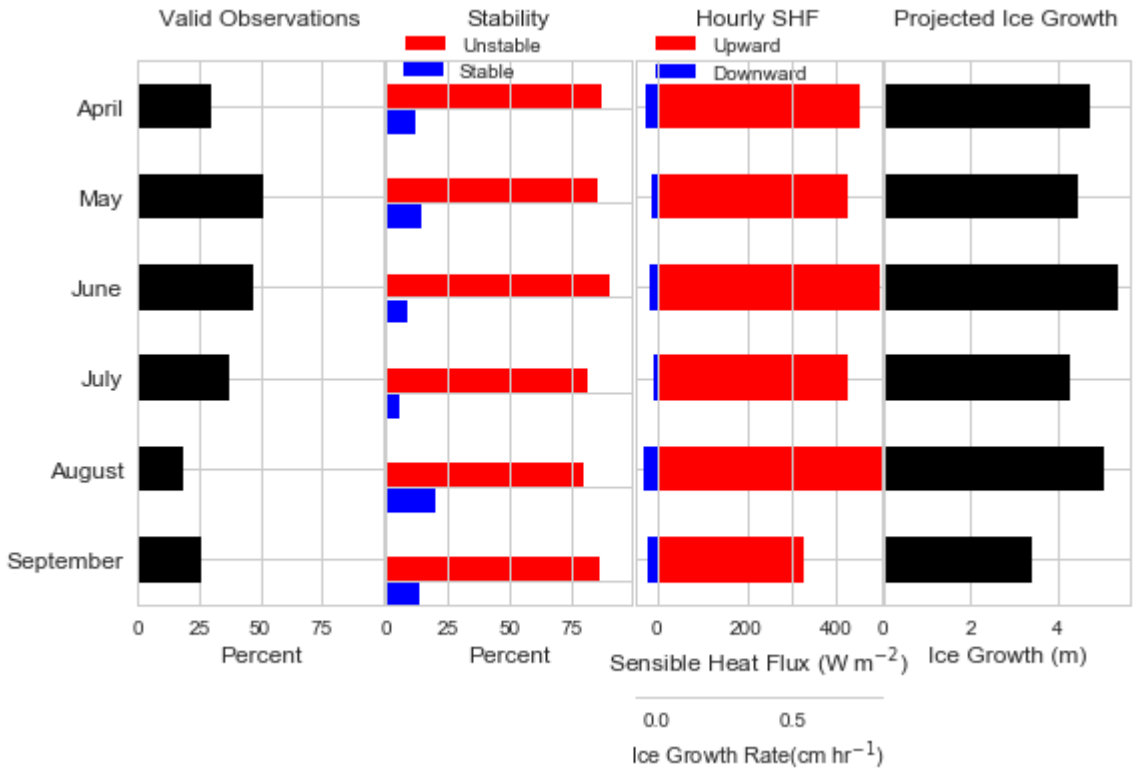

Figure 7: Bar charts representing the monthly variation in the percentage of data valid, the stability conditions with unstable conditions in red and stable conditions in blue, the hourly sensible heat flux in W m^{-2} and ice growth rate in cm h^{-1} with red representing upward (positive) fluxes and blue representing downward (negative) fluxes and the seasonal ice growth in m.

(Figure 7) than with downwind distance (Figure 5), with values ranging from 9.3 W m^{-2} in July to 31.8 W m^{-2} in August.

Chapter 5

Summary

AWS temperature and wind speed and satellite surface temperature observations from Terra Nova Bay are compiled for the winter seasons of 2003, 2005, and 2012-2017 and used as input in the COARE algorithm to calculate sensible heat fluxes over the Terra Nova Bay polynya. The fluxes are analyzed using Spearmans Rank Correlation to quantify the relationships between the sensible heat flux and the atmospheric and surface parameters that are used to calculate the fluxes. The strongest relations are found to be that of the sensible heat flux and wind speed and sensible heat flux and air-surface temperature difference. The sensible heat fluxes are calculated at three downwind distances from the coast to examine the sensible heat flux response to changing atmospheric and surface conditions. The changing surface temperature was found to have the largest impact on the downwind changes in sensible heat flux. The upward sensible heat flux decreases from an average of 457.8 W m^{-2} to 163.56 W m^{-2} over the 30 km distance from the coast that was analyzed. This corresponds to a seasonal ice growth of 30 m at the coast decreasing to 9 m at 30 km downwind from the coast. Hourly upward sensible heat flux values range from 328.9 W m^{-2} to 511.0 W m^{-2}. With the exception of September (hourly ice growth of 0.5 cm h^{-1}), the sensible heat fluxes convert to hourly ice growth rates ranging from 0.7 to 0.8 cm h^{-1}. This results in an estimate of 4 to 5 m of projected monthly ice production.

Bibliography

[Cassano et al., 2010] Cassano, J. J., Maslanik, J. F., Zappa, C. J., L.Gordon, A., Cullather, R. I., and Knuth, S. L. (2010). Observations of Antarctic polynya with unmanned aircraft systems. EOS, 91.

[Cassano et al., 2016] Cassano, J. J., Seefeldt, M. W., Palo, S., Knuth, S. L., Bradley, A., Herrman, P. D., Kernebone, P. A., and Logan, N. J. (2016). Observations of the atmosphere and surface state over Terra Nova Bay, Antarctica using unmanned aircraft systems. Earth System Science Data, 8:115–126.

[Davolio and Buzzi, 2002] Davolio, S. and Buzzi, A. (2002). Mechanisms of antarctic katabatic currents near terra nova bay. Tellus A, 54:187–204.

[Fairall et al., 1996] Fairall, C. W., Bradley, E., Rogers, E. P., Edson, J. B., and Young, G. S. (1996). Bulk parameterizations of air-sea fluxes for TOGA COARE. Journal of Geophysical Research, 101:3747–3764.

[Fairall et al., 2003] Fairall, C. W., Bradley, E. F., Hare, J. E., Grachev, A. A., and Edson, J. B. (2003). Bulk parameterizations of air-sea fluxes for TOGA COARE: Updates and verification for the coare algorithm. Journal of Climate, 16:571–591.

[Fusco et al., 2002] Fusco, G., Flocco, D., Budillon, G., Spezie, G., and Zambianchi, E. (2002). Dynamics and Variability of Terra Nova Bay Polynya. Marine Ecology, 23:201–209.

[Hall and Riggs, 2015a] Hall, D. K. and Riggs, G. A. (2015a). MODIS/Aqua Sea Ice Extent Daily L3 Global 1km EASE-Grid Day, Version 6. h09v31 April 2003 - September 2017. NASA National Snow and Ice Data Center Distributed Active Archive Center.

[Hall and Riggs, 2015b] Hall, D. K. and Riggs, G. A. (2015b). MODIS/Aqua Sea Ice Extent Daily L3 Global 1km EASE-Grid Night, Version 6. h09v31 April 2003 - September 2017. NASA National Snow and Ice Data Center Distributed Active Archive Center.

[Hauser et al., 2002] Hauser, A., Lythe, M., and Wendler, G. (2002). Sea-ice conditions in the Ross Sea during Spring 1996 as observed on SAR and AVHRR Imagery. Atmos.Ocean, 40:281292.

[Knuth and Cassano, 2011] Knuth, S. L. and Cassano, J. J. (2011). An Analysis of Near-Surface Winds, Air Temperature, and Cyclone Activity in Terra Nova Bay, Antarctica, from 1993 to 2009. Journal of Applied Meteorology and Climatology, 50:662–680.

[Knuth and Cassano, 2014] Knuth, S. L. and Cassano, J. J. (2014). Estimating Sensible and Latent Heat Fluxes Using he Integral Method from in situ Aircraft Measurements. Journal of Atmospheric and Oceanic Technology, 31:1964–1981.

[Knuth et al., 2013] Knuth, S. L., Cassano, J. J., Maslanik, J. A., Hermann, P. D., Kernebone, P. A., Crocker, R. I., and Logan, N. J. (2013). Unmanned aircraft system measurements of the atmospheric boundary layer over Terra Nova Bay, Antarctica. Earth System Science Data, 5:57–59.

[Kurtz and Bromwich, 1985] Kurtz, D. D. and Bromwich, D. H. (1985). A recurring, atmospherically forced polynya in Terra Nova Bay. Antarctic Research Series, 43:177–201.

[Lazzara et al., 2012] Lazzara, M. A., Weidner, G. A., Keller, L. M., Thom, J. E., and Cassano, J. J. (2012). ANTARCTIC AUTOMATIC WEATHER STATION PROGRAM: 30 years of Polar Observations. Bulletin of the American Meteorological Society, pages 1519–1537.

[Martin and Kauffman, 1981] Martin, S. and Kauffman, P. (1981). A Field and Laboratory Study of Wave Damping by Grease Ice. Journal of Glaciology, 27:283–313.

[Ohshima et al., 2016] Ohshima, K. I., Nihashi, S., and Iwamoto, K. (2016). The role of katabatic winds on the antarctic surface wind regime. Geoscience Letters, 3.

[Ono, 1967] Ono, N. (1967). Specific Heat and Heat of Fusion of Sea Ice. International Conference on Low Temperature Science. I. Conference on Physics of Snow and Ice, II. Conference on Cryobiology.

[Parish and Bromwich, 2007] Parish, T. R. and Bromwich, D. H. (2007). Reexamination of the Near-Surface Airflow over the Antarctic Continent and Implications on Atmospheric Circulations at High Southern Latitudes. Monthly Weather Review, 135:19611973.

[Parish and Cassano, 2003] Parish, T. R. and Cassano, J. J. (2003). The role of katabatic winds on the Antarctic surface wind regime. Monthly Weather Review, 131:317–333.

[Sansiviero et al., 2017] Sansiviero, M., Maqueda, M. M., Fusco, G., Aulicino, G., Flocco, D., and Budillon, G. (2017). Modelling sea ice formation in the Terra Nova Bay polynya. Journal of Marine Systems, 166:4–25.

[Scambos et al., 2006] Scambos, T. A., Haran, T., and Massom, R. (2006). Validation of AVHRR and MODIS ice surface temperature products using in situ radiometers. Annals of Glaciology, 44:345351.